Original scientific paper

COMBINED EFFECTS OF ELECTROSTATIC AND ELECTROMAGNETIC INTERFERENCES OF HIGH VOLTAGE OVERHEAD POWER LINES ON AERIAL METALLIC PIPELINE

Djekidel Rabah[1], Mohamed Lahdeb[1], Sherif Salama M. Ghoneim[2], Djillali Mahi[1]

[1]Laboratory for Analysis and Control of Energy Systems and Electrical Systems LACoSERE, Laghouat University (03000), Algeria
[2]Electrical Engineering Department, College of Engineering, Taif University, P.O. Box 11099, Taif 21944, Saudi Arabia

Abstract. *The main purpose of this paper is to model and analyze the electrostatic and electromagnetic interferences between a HV overhead power line and an aerial metallic pipeline situated parallel at a close distance. The modelling of these interferences is typically done for safety reasons, to ensure that the induced voltage does not pose any risk to the operating and maintenance personnel and to the integrity of the pipeline. The adopted methodologies respectively for electrostatic and electromagnetic interferences are based on the charge and current simulation methods combined with the Teaching learning based optimization (TLBO) algorithm. The Friedman test analysis indicate that teaching learning based optimization (TLBO) algorithm can be used for parameters optimization, it showed better results. In the case where the induced currents and voltages values exceed the limit authorized values by the international CIGRE standard, mitigation measures become necessary. The simulation results obtained were compared with those provided respectively by the admittance matrix analysis and Carson's method, good agreement was obtained.*

Key words: *Charge Simulation Method (CSM), Current Simulation Technique (CST), Teaching Learning Based Optimization (TLBO), Friedman Test, HV power line, Aerial Metallic Pipelines*

Acronyms:

AC	Alternating Current	FEM	Finite Element Method
CIGRE	International Council on Large Electric Systems	GA	Genetic Algorithm
		HS	Harmony Search
CSM	Charge Simulation Method	HV	High Voltage
CST	Current Simulation Technique	IEEE	Institute of Electrical and Electronics Engineers
DC	Direct Current		
EAs	Evolutionary algorithms	NNA	Nodal Network Analysis
EMF	Electromotive Force	OF	Objective Function
FBA	Flower Pollination Algorithm	PSO	Particle Swarm Optimization
FDM	Finite Difference Method	TLBO	Teaching Learning Based Optimization

1. INTRODUCTION

The hydrocarbon and water transport metallic pipelines (buried or aerial) that share common right-of-way with high-voltage overhead transmission power lines network are subject to the influence of electrostatic and electromagnetic interferences created by the electric and magnetic fields emitted by these HV power lines in normal operating condition. These fields can induce voltages and currents in the metallic pipelines installed in the immediate vicinity of these HV power lines. In some cases, these induced voltages can reach to high levels enough to be hazardous to the safety of operating personnel coming into contact with the metallic pipeline, causing severe damage to metallic pipeline safe operation and associated equipment, cathodic protection systems and the pipeline itself [1-4]. Consequently, the induced voltages on the metallic pipelines must be reduced to acceptable levels for the safety of workers personnel, and to ensure the integrity of the pipeline. Based on the above, it is important and necessary to assess electrostatic and electromagnetic interference between transmission power lines and pipelines for performance and safety reasons in normal operation condition of the electric network.

Interference problems involving HV overhead power lines and metallic pipelines have been commonly deal in the literature, where several important researches have been devoted to evaluating the inductive and capacitive interference phenomenon based on various analytical and numerical methods. Different simulation methodologies have been used [5,6], which are generally relied on transmission line approach [7-15], or by finite element method (FEM) alone [16-20], or in combination with circuit analysis [21-26]. In addition, the nodal network analysis [27,28], the finite difference method (FDM) [29,30] and the charge simulation method (CSM) [31-35]. The transmission line approach utilizes Thevenin equivalent circuits as its basic assumption and provides almost good results for the induced voltage, the finite element method (FEM) is a most robust approach with reliable and accurate results for calculating induced voltage, the circuit theory approach gives more conservative results because it does not take into account the effects of infinite transmission line length, the nodal network analysis (NNA) can predict the induced voltage with sufficient accuracy, the finite difference method (FDM) is sufficiently rigorous, leading to accurate results, the charge simulation method (CSM) is one of the most widely used approaches for its various advantages of optimization and accuracy which leads to better accuracy of results.

This present paper proposes a numerical modeling analysis of electrostatic and electromagnetic couplings between HV overhead power lines and a proximity aerial metallic pipeline using hybrid simulation methods. The computation methodologies used were successively designed on the basis of the charge simulation method (CSM) and the current

simulation technique (CST) [36-38]. The main constraints of these analysis methods consist respectively in the number and position of the fictitious charges and the line current filaments. For solving this associated optimization problem in order to obtain the optimal values of these parameters, which provide a solution of sufficient precision of these couplings, Evolutionary computation algorithms (EAs) are commonly used. Evolutionary algorithms (EAs) are stochastic optimization methods based on a rough simulation of the natural evolution of populations. One of the most important and best types of evolutionary algorithms is teaching learning based optimization (TLBO).

The Teaching Learning Based Optimization (TLBO) is a new stochastic optimization meta-heuristics that was originally proposed by Rao et al in 2011[39]. This population search algorithm is inspired by the teaching learning process and is based on the effect of the influence of a teacher on the production of students in a classroom; it is widely used due to their best performance, its efficiency and simplicity of implementation [40]. It has been successfully applied to solve optimization problems in many scientific applications and techniques in recent years.

Finally, the validity of the simulation results obtained by the two proposed combined methods is demonstrated by a comparison with those yielded respectively by the analytical approaches based on the admittance matrix analysis and Carson's equations [15,35].

2. COUPLING MECHANISMS

In electricity, coupling is the transfer of energy from element to another element of the electrical system. There are mainly three types of couplings by which alternating voltages and currents can be induced on metallic pipelines near HV power transmission lines, these sources of interference are electrostatic, electromagnetic and conductive coupling.

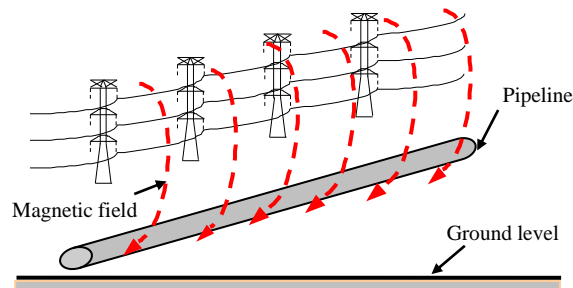### 2.1. Electrostatic Coupling from HV Power Line to Pipeline

Only metallic pipeline installed above ground level is subject to the electrostatic coupling, the buried pipeline is protected by the good shielding effect caused by the ground. If a pipeline is located near a HV power line above ground level, it can undertake a large voltage to ground. The voltage is due to the charges accumulation through the capacitance between the HV power line conductors and pipeline in series with the capacitance between the pipeline and ground, which form a capacitive voltage divider; this is illustrated in Figure 1[1-3].
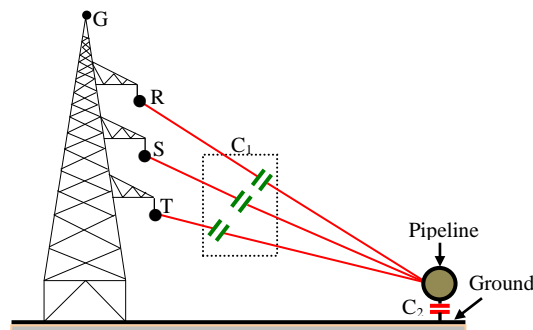
Fig. 1 Electrostatic coupling from HV power line to a metallic pipeline

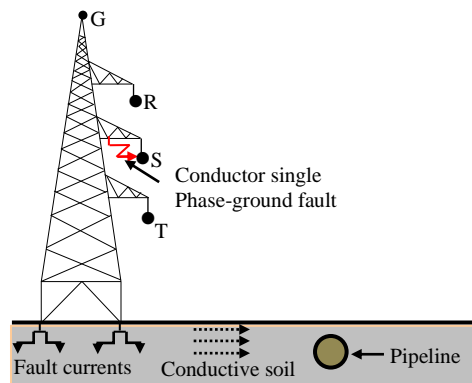## 2.2. Electromagnetic Coupling from HV Power Line to Pipeline

The electromagnetic interference is the result of the magnetic field temporal variation generated by the HV power lines, as shown in Figure 2. Aerial and buried pipelines running parallel to or in close proximity to HV transmission lines are subjected to induced voltages by the time varying magnetic flux produced by the HV transmission line currents according to Faraday's law of electromagnetic induction. The induced voltage causes currents circulation on the pipeline and voltages between the pipeline and the surrounding earth [1-3].

Fig. 2 Electromagnetic coupling from HV power line to a metallic pipeline

2.3. Conductive Coupling from HV Power Line to Pipeline

Conductive coupling appears when a phase-to-earth or phase-to-phase-to-earth default had occurred. In this case, a large amount of current flows to earth through the pylon earthing, as shown in Figure 3 below. This current raises the ground potential in proximity to metallic pipeline. This high voltage stresses the coating of pipelines and can cause arcs that damage the pipeline coating or the pipeline itself. In addition, this high voltage difference could pose an electric shock hazard to person directly touching the pipeline [1-3].

Fig. 3 Conductive coupling from HV power line to a metallic pipeline

3. ELECTROSTATIC COUPLING CALCULATION

Charge simulation method (CSM) is a numerical calculation tool for the solution of boundary value problems of Laplace's equation. This method was initially proposed by Steinberger in 1969 [41], and then it was well developed and turned into a very powerful and efficient tool for calculating the electric field for high-voltage equipment. In fact, this method is very simple to use and implement; it can quickly deal with the problem to be solved while providing an accurate solution [42, 43-45].

In the principle of this method, each conductor is simulated by a number of simulated fictitious infinite line charges placed inside the conductor around a cylinder of fictitious radius. In most problems concerning the solution by the charge simulation method (CSM), there is a plane of symmetry which is generally represented by the earth conventionally assumed that its reference potential is zero, this procedure makes it possible to take into account the ground effect, by introducing the concept of image charges [46-50]. Therefore, the number of boundary points selected on the conductor's surface is assumed to be equal to the number of simulated charges; these charges are placed in such a manner while satisfying the Dirichlet type boundary conditions. Once the magnitudes of these simulated charges are determined, the potential at any point in space outside the region of the conductors can be determined using the superposition theorem as follows [50-53]:

$$V_i = \sum_{j=1}^{n_c} P_{ij} \times q_j \tag{1}$$

Where, n_c is the total number of simulated charges; P_{ij} is the Maxwell's potential coefficient at the contour point (i) created by the simulated charge q_j.

Firstly, the magnitudes of simulated charges are computed by solving the system of n_c linear equations for n_c unknown charges in the form described below in Equation (2) [50-53]:

$$[q_j]_{n_c} = [P_{ij}]^{-1}_{n_c \times n_c} \times [V_{ci}]_{n_c} \tag{2}$$

Where, q_j is the column vector of the simulated charges on the conductors; V_{ci} is the column vector of the known potentials at the boundary points of the conductors; P_{ij} is the matrix of the Maxwell potential coefficients of the conductors.

As an example, in Figure 4, we consider three point charges in free space placed at different distances from the point M_i. According to the superposition principle, the potential V_i at this point will be [41]:

$$V_i = \frac{q_1}{4\pi\varepsilon_0 R_1} + \frac{q_2}{4\pi\varepsilon_0 R_2} + \frac{q_3}{4\pi\varepsilon_0 R_3} = P_{i1} q_1 + P_{i2} q_2 + P_{i3} q_3 \tag{3}$$

Once the magnitudes of the simulated charges are calculated after solving the system of Equation (2), it is necessary to check whether these calculated magnitudes produce the same real boundary conditions fixed on the conductors' surface; in order to get the best calculation precision. Firstly, by selecting several checkpoints around the conductors, the new potential can be computed by these checkpoints on the surface of conductors. Secondly, by determining the relative error between the new calculated potential and the real potential applied to the contours of the conductors, which makes it possible to indicate the simulation accuracy. If this accuracy does not satisfy the simulation criterion, it is necessary to change the number and/or location of the simulated charges. Once this is done, the electric field strength at any point can be computed [50-53].
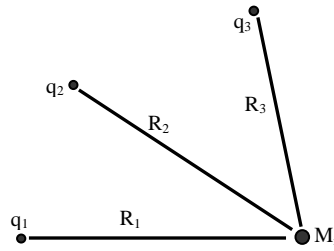
Fig. 4 Three point charges in free space

The charge simulation method (CSM) is widely used to calculate the electric field strength in the vicinity of very high voltage overhead transmission lines. Generally, the type of charges used for overhead power lines are of infinite length, because the radius of the conductor is negligible compared to its length. The typical emplacement of simulated charges and contour points in the conductor/pipeline cross-section is shown in Figure 5.

●: Simulated charges
o : Contour points
★ : Check point
r1: Real radius of the conductor/pipeline
r2: Fictitious radius of the conductor/pipeline
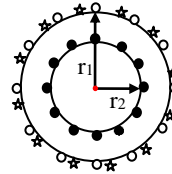
Fig. 5 Two-Dimensional arrangement of simulation charges and contour points for the line conductor and the pipeline

The general form of coordinates for contour points and simulated charges along the orthogonal frame is described by the following equations [35,36,51]:

$$x_k = x_0 + R \times \cos\left(\frac{2\pi}{n_k} \times (k-1)\right) , \quad y_k = y_0 + R \times \sin\left(\frac{2\pi}{n_k} \times (k-1)\right) \quad (4)$$

Where, $R = r_1$ if $k = i$, r_2 if $k = j$, y_0 is the height of conductors/ pipeline above ground level; x_0 is the horizontal coordinates of conductors/ pipeline.

The electric field calculation generated by an electric charge is described by Gauss's Law. For a three-phase transmission line, in a rectangular coordinate system, the horizontal and vertical components of the electric field intensity along the two perpendicular axes due to all the simulated charges, including the image charges, are expressed by the equations described below [50-53]:

$$E_{x_i} = \sum_{j=1}^{n_c} f_{ij}\, q_j \ , \quad E_{y_i} = \sum_{j=1}^{n_c} f_{ij}\, q_j \quad (5)$$

Where, f_{x_i} and f_{y_i} are the electric field intensity coefficients between the contour points and the simulated charges q_j.

The total electric field strength at any observation point is calculated as follows [43]:

$$E_{res} = \sqrt{E_{xi}^{\,2} + E_{yi}^{\,2}} \quad (6)$$

The induced voltage on the aerial metallic pipeline due to the capacitive effect of all electrical charges that simulate the conductors is evaluated as follows [1,33]:

$$V_{ind} = \frac{1}{2\,\pi\,\varepsilon_0} \sum_{j=1}^{n_c} q_j . \ln\left(\frac{\sqrt{(x-x_j)^2 + (y+y_j)^2}}{\sqrt{(x-x_j)^2 + (y-y_j)^2}} \right) \tag{7}$$

Where, (x,y) are the coordinates of the observation point; (x_j, y_j) are the coordinates of the simulated charges.

If a person is in contact with the ground and at the same time touches this pipeline, he gets an electric shock whose current passing through his body is given by the following relationship [1, 32]:

$$I_{shock} = j\,\omega\,C_p\,L_p\,V_{ind} \tag{8}$$

Where, L_p is the length of the pipeline exposed to the electrostatic coupling; C_p is the pipeline's capacitance to earth per unit length; ω is the angular frequency.

When the discharge current in human body exceeds the safe limit in steady state conditions defined by the CIGRE standard at 10 mA [1], its reduction below the admissible level is required; the best protection is to connect the metallic pipeline to the ground through an adequate resistance R_g, its value must be less than [1,54]:

$$R_g \prec \frac{R_{body}}{\beta - 1} \tag{9}$$

Where, R_{body} is the body resistance; β is a ratio which is given by $\beta = (I_{shock} / I_{adm})$.

According to the American standard IEEE 80:2013, the overall resistance of the human body is usually taken equal to 1000 Ω [1,55].

3. ELECTROMAGNETIC COUPLING CALCULATION

Many analytical and numerical methods are available for modeling and simulating magnetic induction due to very high voltage (VHV) overhead transmission lines. The current simulation technique (CST) is the most suitable method for two-dimensional computation, as it represents a reliable and efficient evaluation tool in the numerical solution of the magnetic induction equation for open boundary problems. Its basic principle is very similar to that of the charge simulation method (CSM) [37, 38]. High voltage transmission lines may use the bundled conductors (multiple sub-conductors per phase) to increase the electrical transport capacity. This approach consists by representing each current passing through a sub-conductor by a set of finite number of current filaments n_f. In this method, each current passing through a sub-conductor is considered as a set of finite number of current filaments n_f, which are allocated across a cylinder surface of fictitious radius R_j. In a three-phase transmission line with bundled conductors, if each phase conductor consists of (m) identical sub-conductors, the total number of sub-conductors is ($3{\times}m$), as shown in Figure 6. The number and position of simulated filament currents depends on the total number of power line conductors, their spatial arrangements and boundary conditions.

For the full number of currents filaments line, the simulation currents along the all sub-conductors I_i ($i = 1.......3{\times}n_f{\times}m$) must satisfy the following conditions [56-59]:

1 - The normal component of the magnetic field intensity on the sub-conductor surfaces is zero, according to the Biot-Savart's law.

2 - The sum of the filamentary currents which simulates the current in the sub-conductor must be equal to the real current passing through the sub-conductor.

After selecting several contour points on the sub-conductors surface, the unknown simulation currents can be assessed by solving the system of equations given below:

$$A_{ij} = \sum_{i=1}^{3\,n_f\,m} K_{ij}\,I_i = 0 \; , \; j = 1, 2, 3, ...,3\,m\,(n_f - 1) \tag{10}$$

$$\sum_{i=(q-1)n_f+1}^{n_f\,q} I_i = I_{cq} \; , \; q = 1, 2, 3, ...,3\,m \tag{11}$$

Where, m is the number of sub-conductors per phase; n_f is the number of filament line currents; K_{ij} is the coefficient of normal magnetic field defined by the coordinates of the ith contour point and the jth filament line current, it is given by [37,38]:

$$K_{ij} = \frac{\mu_0}{2\pi} \ln \frac{R_j}{R_{ij}} \tag{12}$$

Where, R_{ij} is the distance between the simulation current point (j) and the contour point (i) at sub-conductor surface, R_j is the fictitious radius of current filament simulation (see Figure 7).
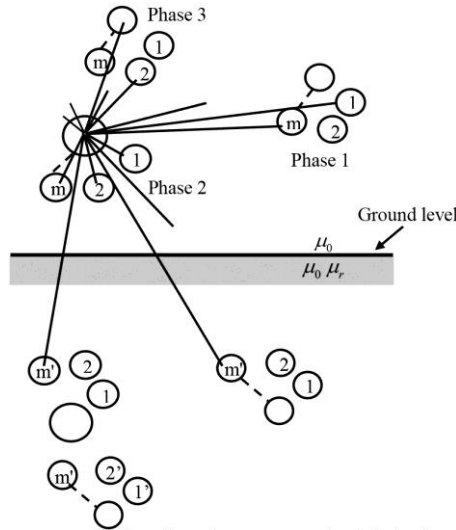

Fig. 6 Three phase transmission line above ground with the images of line conductors
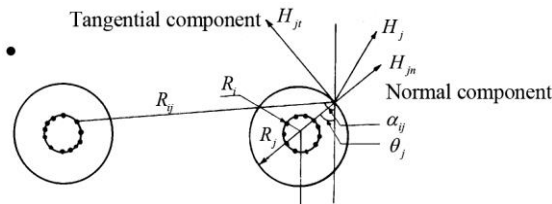

Fig. 7 Normal and tangential field components at a point on the sub-conductor surface

Having calculated the values of the current line filaments by solving the equations system mentioned above in Equations (10) and (11). It can be checked about the values and position of the currents filaments by adopting the same steps mentioned above in the charge simulation method (CSM). In quasi-static analysis, the magnitude of the magnetic induction B is derived from the curl of the vector potential A, thus, the horizontal and vertical components of the magnetic induction vector according to the two perpendicular axes (x and y) can be determined as follows [37,38]:

$$\vec{B} = \nabla \times \vec{A} \implies B_{xi} = \frac{\partial A_{ij}}{\partial x} \quad and \quad B_{yi} = \frac{\partial A_{ij}}{\partial y} \tag{13}$$

Where, A_{ij} is the magnetic potential generated by the HV power line conductors' currents, it can be expressed by the following relation [37,38]:

$$A_{ij} = \frac{\mu_0}{2\pi} \sum_{i=1}^{3nm} I_i K_{ij} \tag{14}$$

In this magnetic induction calculation, taking into account the earth effect. The induced currents in the earth represented by the filament image currents, which are located at a depth of penetration D_e below the surface of the earth, it can be calculated using the formula below [37,38]:

$$D_e = 658.87 \sqrt{\frac{\rho_s}{f}} \tag{15}$$

Where, ρ_s is the electrical resistivity of the soil; f is the frequency of the source current.

Finally, the resulting magnetic induction intensity at a given point in space can be obtained by adding the horizontal and vertical components mentioned above in Equation (13), as indicated below [37,38]:

$$B_{res} = \sqrt{B_{xj}^2 + B_{yj}^2} \tag{16}$$

Also, in this magnetic induction calculation, it is desirable to take into account the effects of induced currents circulating in the earth wires and metallic pipeline, which are caused by the three-phase currents passing through the phase conductors, they can be calculated by the following expression [60,61]:

$$[I_g] = -[Z_{gg}]^{-1} [Z_{gc}] [I_c] \tag{17}$$

Where, Z_{gg} are the self impedances of the earth wires and metallic pipeline; Z_{gp} are the mutual impedances between the phase conductors and earth wires / metallic pipeline; I_c are the currents passing through the three-phase conductors of the power line; I_g represents the induced currents in the earth wires and metallic pipeline.

In the Extremely Low Frequency domain, the self and mutual longitudinal impedances of the conductors with ground return can be obtained by the simplified formulas of Carson-Clem as shown below, respectively [60,61]:

$$Z_{gg} = R_g + \frac{\mu_0 \omega}{8} + j \frac{\mu_0 \omega}{2\pi} [\ln(\frac{D_e}{R_{GM}})] \tag{18}$$

$$Z_{gc} = \frac{\mu_0 \omega}{8} + j \frac{\mu_0 \omega}{2\pi} \ln(\frac{D_e}{d_{gc}}) \tag{19}$$

Where, R_g is the DC conductor resistance, R_{GM} is the geometric mean radius of the conductor; d_{gc} is the mutual distance between two conductors; ω is the angular frequency; D_e is the penetration depth of earth return; μ_0 is the permeability of free space.

The induced voltage on the aerial metallic pipeline due to the magnetic effect can be calculated through Faraday's Law of electromagnetic induction. This law explains that magnetic induction that changes with time will induce a voltage in the pipeline; the total flux ϕ_t due to all currents flowing through the conductors and change with time onto the pipeline is calculated as a surface integral as shown in [62-64].

$$\phi_t = \int_S \vec{B}_{res}\, d\vec{S} \tag{20}$$

Where, ϕ_t is the total flux density produced by all power line conductors; S is the total surface area.

The metallic pipeline conductors form a closed loop, they are located at the position of the coordinates as shown in Figure 8, the total magnetic flux ϕ_t flowing through the surface S defined by the set of coordinates of the power line conductors and the pipeline can be expressed as following [62-64]:

$$\phi_t = -\frac{\mu_0\, L}{4\,\pi} \sum_1^n I_i \ln \frac{(x_p + x_i)^2 + (y_p + D_e + y_i)^2}{(x_p + x_i)^2 + (y_p - y_i)^2} \tag{21}$$

Where, (x,y) are the coordinates of the power line conductors; (x_j,y_j) are the coordinates of the metallic pipeline.

Finally, using the total magnetic flux, the induced voltage on the metallic pipeline due to the magnetic coupling can be expressed as follows [62-64]:

$$V_{ind} = -\frac{\partial \phi_t}{\partial t} = -j\,\omega\,\phi_t \tag{22}$$

In case of direct accidental contact with the metallic pipeline, the value of the shock current flowing through the human body can be calculated by this equation below [15,55]:

$$I_{shock} = \frac{V_{ind}}{Z_{pipe} + R_{body} + R_c} \tag{23}$$

Where, R_{body} is the human body resistance; R_c is the ground contact resistance of a person; Z_{pipe} is the total impedance of the metallic pipeline, it is calculated by the equation given below [1]:

$$\frac{\sqrt{\rho_p\,\mu_p\,\mu_0\,\omega}}{\sqrt{2}\,\pi\,D_p} + \frac{\mu_0\,\omega}{8} + j\,[\,\frac{\sqrt{\rho_p\,\mu_p\,\mu_0\,\omega}}{\sqrt{2}\,\pi\,D_p} + \frac{\mu_0\,\omega}{2\,\pi} \ln(\frac{3,7\sqrt{\rho_s\,\omega^{-1}\,\mu_0^{-1}}}{D_p})\,] \tag{24}$$

Where, D_p is the pipeline's diameter; μ_p is the relative permeability of the pipeline's metal; ρ_p is the pipeline's resistivity.
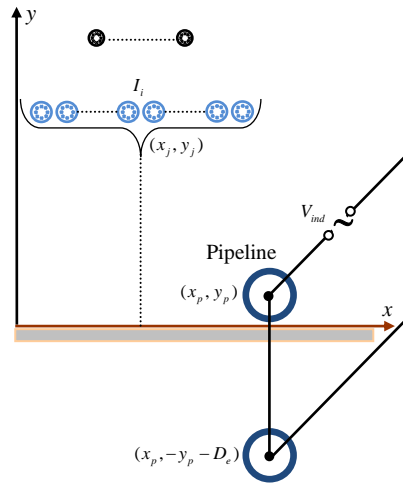
Fig. 8 Determination of the induced voltage on the metallic pipeline

For touch voltages, for a soil with a surface resistivity, the contact resistance R_c is calculated as [15]:

$$R_c = 3,125 \times \rho_s \tag{25}$$

In some cases, the induced voltage exceeds the acceptable limit recommended by international standards; the international CIGRE regulations insist that safety measures be taken into account if the voltage on the pipeline exceeds 50V in steady state [1]. In this case, the mitigation is necessary to maintain the voltage within the permitted limit; it is enough to connect the metallic pipeline to the ground with two identical electrodes at each end of the pipeline.

4. TEACHING LEARNING BASED OPTIMIZATION (TLBO)

Teaching learning based optimization (TLBO) is a meta-heuristic optimization algorithm proposed by Rao et al. [39]. This is inspired from the teaching-learning process and is based on the effect of a teacher's influence on the output of students in a classroom environment. The teacher-students interaction is the fundamental inspiration for this algorithm, a group of learners in a classroom is considered as a population size and the different subjects offered to the learners are similar to the different design variables of the optimization problem. The results of the learner are analogous to the objective function value of the optimization problem, and the number of exams is the number of iterations, the best solution in the whole population is considered the teacher. The major advantage of this algorithm is the fact that it does not require specific control parameters. The teacher and the learners are the two essential components of the algorithm, thus, this algorithm describes two learning processes, through teacher (known as the teacher phase) and through interaction with other learners (known as the learner phase) [65-70].

4.1. Teacher Phase

During this phase, the teacher aims to impart knowledge to the learners and tries to improve the average result of the classroom, making the maximum efforts to increase the level of knowledge of those learners who acquire his knowledge depending on the quality of the teaching provided by this teacher and the skills of the learners present in the class. Taking this into account, the difference between the teacher's result and the learner's average result in each subject is expressed as follows [65-70]:

$$Diff_i = r_i(X_{T,i} - T_F \times M_i) \tag{26}$$

Where, r_i is a random number in [0, 1]; TF is a random number that accounts for the teacher factor that depends on teaching quality, and equals either 1 or 2. The value of TF is calculated at random by the following formula [65-70]:

$$T_F = round \ [1 + rand(0,1)\{1,2\}] \tag{27}$$

Through the processes of teaching and transferring knowledge to learners and their acquisition, their new results being modified in the upcoming test, this difference is represented by the following expression [65-70]:

$$X'_{j,i} = X_{j,i} + Diff_i \tag{28}$$

Where, $X'_{j,i}$ and $X_{j,i}$ are the new and old grades learner (j) earned in exam (i), respectively.

The best result among the two possible will be accepted and to be used as input for the learner phase.

4.1. Learner Phase

In this second phase, the learners increase their knowledge through the interaction between them, also by discussing and interacting with other better learners by working as a collective team which helps to produce the best results X''. Considering a population size of N, the helping interaction learning phenomenon between two learners A and B in each exam for minimization problems is explained as follow [65-70]:

$$X''_{A,i} = \begin{cases} X'_{A,i} + r_i(X'_{A,i} - X'_{B,i}) \ if \ (X'_{A,i} \succ X'_{B,i}) \\ X'_{A,i} + r_i(X'_{B,i} - X'_{A,i}) \ if \ (X'_{B,i} \succ X'_{A,i}) \end{cases} \tag{29}$$

X'' is accepted into the population if it gives a better function value.

The implementation steps of TLBO algorithm can be summarized as follows [71-73]:

Step 1: Define the optimization problem (minimization) and initialize the parameters of algorithm, the population size, number of variables, the maximum number of iterations, and the objective function $f(X)$.

Step 2: Randomly initialize the grades (solutions) ($X_{i,j}$) of n learners (j = 1, 2, ..., n) in exam (i = 1).

Step 3: Calculate the objective function for n students in exam (i)

Step 4: Calculate (M_i) and ($X_{T,i}$), identify the best solution as teacher according to $X_{teacher} = X_{f(X)=\min}$

Step 5: Calculate $Diff_i$ for exam (i) according to Equation (26) by utilizing the teaching factor T_F.

Step 6: Calculate $X'_{j,i}$ for n learners in exam (i) according to Equation (28), compare the two solutions $X'_{j,i}$ and $X_{j,i}$, accept the best solution for transferring to the next step.
Step 7: Choose randomly each pair of learners and update the solution according to (4) and accept the better for the next step.
Step 8: Calculate the objective function for all learners, check if the stopping criterion is met (the optimal solution is obtained), otherwise the algorithm will iterate from step (4).

For charge simulation method (CSM), the objective function used for the relative error is very simple and has the form given in the following equation [38]:

$$OF_1 = \frac{1}{n_c} \left| \sum_{i=1}^{n_c} \frac{V_{ci} - V_{vi}}{V_{ci}} \right| \times 100 \tag{30}$$

Where: V_{vi} is the exact potential to which is subjected the conductor and V_{ci} is the actual voltage of the check points; n_c is the total number of check points.

For current simulation technique (CST), the employed objective function is expressed by the relative error of the magnetic potential as follows [38]:

$$OF_2 = \frac{1}{n_f} \left| \sum_{i=1}^{n_f} \frac{A_{ci} - A_{vi}}{A_{ci}} \right| \times 100 \tag{31}$$

Where, A_{ci} is the magnetic potential calculated by the current filaments points; A_{vi} is the new magnetic potential estimated by the matching filaments points; n_f is the total number of matching points.

5. FRIEDMAN'S STATISTICAL TEST

In fact, to prove the superiority and the best performance of an optimization algorithm in comparison with the analytical results obtained by different algorithms, we most often use the Friedman nonparametric test to determine if the algorithms are statistically different and to classify them in terms of performance and speed, in order to implement the best of them in the optimization problem. Generally, to conclude on the result of a statistical test, the procedure employed consists in quantifying the p-value and compare it to a previously defined threshold (traditionally 5%). If the p-value is less than this threshold, the null hypothesis is rejected in favor of the alternative hypothesis, and the test result is declared statistically significant [74-77].

In this paper, the Friedman's statistical test will be used to analyze the minimum values of the objective function obtained from different optimization algorithms such as the teaching learning based optimization (TLBO) [78], flower pollination algorithm (FPA) [79], harmony search algorithm (HS) [80], particle swarm optimization (PSO) and genetic algorithm (GA) [81], in order to identify the most efficient algorithm.

6. VALIDATION METHODS

In case of electrostatic coupling, the induced voltage on the metallic pipeline caused by the HV power line conductors can be evaluated using the admittance matrix technique. Under steady-state operation condition, for a symmetrical HV overhead transmission power

line system with an aerial metallic pipeline, the shunt admittance matrix per unit length of the proposed electric circuit is determined by the following equation [1,54,82-85].

$$[Y_{ij}] = j\,\omega\,[P_{ij}]^{-1} \tag{32}$$

Where, P_{ij} is the potential coefficients matrix of the proposed circuit (overhead power line conductors and metallic pipeline).

Then the current-voltage relations for this electric system can be represented in matrix form as follows:

$$[I_i] = [Y_{ij}][V_i] \tag{33}$$

The resulting matrix of shunt admittances for the total number of conductors (including three-phase conductors, earth wires and metallic pipeline) is represented below [1,53,81-85]:

$$\begin{bmatrix} I_c \\ I_p \\ I_g \end{bmatrix} = \begin{bmatrix} Y_{cc} & Y_{cp} & Y_{cg} \\ Y_{pc} & Y_{pp} & Y_{pg} \\ Y_{gc} & Y_{gp} & Y_{gg} \end{bmatrix} \begin{bmatrix} V_c \\ V_p \\ V_g \end{bmatrix} \tag{34}$$

Where, c, p and g are subscripts which represent respectively the three-phase conductors, metallic pipeline and earth wires.

The current through the earthed earth wires is equal to zero; they can be removed by replacing ($I_g = 0$) in Equation (34), which gives:

$$\begin{bmatrix} I_c \\ I_p \end{bmatrix} = \begin{bmatrix} Y_{cc}^{'} & Y_{cp}^{'} \\ Y_{pc}^{'} & Y_{pp}^{'} \end{bmatrix} \begin{bmatrix} V_c \\ V_p \end{bmatrix} \tag{35}$$

Where,

$$Y_{cc}^{'} = Y_{cc} - \frac{Y_{cg} Y_{gc}}{Y_{gg}}, \; Y_{cp}^{'} = Y_{cp} - \frac{Y_{cg} Y_{gp}}{Y_{gg}} \\ Y_{pc}^{'} = Y_{pc} - \frac{Y_{pg} Y_{gc}}{Y_{gg}}, \; Y_{pp}^{'} = Y_{pp} - \frac{Y_{pc} Y_{cp}}{Y_{gg}} \tag{36}$$

For an insulated metallic pipeline, the current flowing through it is zero $I_p = 0$, by substituting it in Equation (35), the resulting pipeline voltage to earth due to the electrostatic coupling with the HV power line can easily be deduced and given by the following relation [1,53,81-85]:

$$[V_p] = -[Y_{pc}^{'}]^{-1}[Y_{pp}^{'}][V_c] \tag{37}$$

Where, V_c is the column of the known three-phase voltages to earth of the HV power line conductors.

In electromagnetic coupling case, under steady state conditions, the induced voltage on the metallic pipeline can be obtained by applying Carson's method. This approach is based on the principle of mutual impedances between the conductors of the HV power line and the metallic pipeline, the determination of these impedances is done using Carson's formula mentioned previously in Equation (19) [4,85-90].

The induced voltage calculation that appears between the metallic pipeline and the adjacent earth is done in two steps, firstly, the determination of the electromotive force (EMF) induced along the metallic pipeline due to variable magnetic field, and then the induced voltage along the metallic pipeline can be obtained.

The total longitudinal electromotive force (EMF) induced on the metallic pipeline is obtained through the mutual impedances between the pipeline and the power line conductors, carrying a time varying alternating currents in the power line conductors. In the case where the overhead power line is equipped by one earth wire, the induced electromotive force (EMF) is calculated according to the following equation [4,85-90]:

$$E_{ind} = -I_{c_1} Z_{pc_1} - I_{c_2} Z_{pc2} - I_{c3} Z_{pc3} - I_{g_1} Z_{pg_1} \tag{38}$$

This relation can be easily reduced to the general form below:

$$E_{ind} = -\sum_{i=1}^{n_i} I_i Z_{pi} \tag{39}$$

Where, z_{pi} are the mutual impedances between the conductors of the power line (phase conductors, earth wires) and the metallic pipeline; I_i are the currents passing through the three-phase conductors and the earth wires of the power line; n_i is the total number of conductors in the HV power line.

The induced voltage on the metallic pipeline for an exposed length of exposure L to the electromagnetic coupling can be found using the formula given below [4,85-90]:

$$V_{ind} = E_{ind} L \tag{40}$$

As can be see; this applied approach assumes that the induced voltage is constant over the entire length of the metallic pipeline.

Consider an HV overhead vertical single circuit transmission line of 275 kV, with one earth wire and an aerial insulated metallic pipeline in the immediate vicinity; the arrangement and geometric coordinates of the overhead power line and metallic pipeline are shown in Figure 9. The pipeline is placed in perfect parallel to the axis of the HV power overhead line at a separation distance of 45 m; its height above the ground is 1 m with a radius of 0.3m. The metallic pipeline length of exposure to the AC interference is 25 km. The three-phase currents in HV power line have been assumed under balanced operation with the magnitude of 500 A, with a nominal system frequency of 50 Hz. The earth is assumed to be homogeneous with a resistivity of 100 (Ω m), the AC resistance of the phase conductor is 0.1586 (Ω/km), for the earth wire is 0.1489 (Ω/km) and 0.5 (Ω/km) for the metallic pipeline.
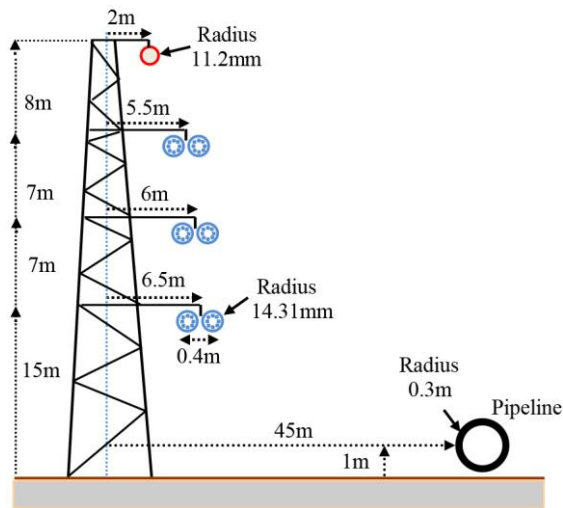
Fig. 9 Single circuit HV vertical configuration with an aerial metallic pipeline

7. RESULTS AND DISCUSSIONS

Firstly, the aim is to select the best parameters to insert in the simulation methods to achieve results with satisfactory accuracy. In order to obtain the optimal number and location of fictitious charges and current filaments, it is necessary to use a robust and powerful optimization algorithm.

In this context, a comparison of the performances of different optimization algorithms (PSO, FBA, HS, TLBO, GA) was made using the statistical Friedman test under the same conditions, in order to be able to classify them according to their performance. To ensure a fair comparison, these algorithms were implemented in the Matlab interface (R2014a), the experiments for each algorithm were repeated 10 times on the same computer running with Windows 10 operating system. Parameter settings of all optimization algorithms are shown in Table 1.

Table 1 Parameters Settings of each algorithm

Algorithms	Parameters Setting (100 iterations)
Particle Swarm Optimization (PSO)	Swarm size N =20; Learning factor c1=2, c2=2; Inertia weight wmax=1.2; wmin=0.4.
Flower Pollination Algorithm (FPA)	Population size N=20; switch probability p=0.8
Harmony Search Algorithm (HS)	Harmony Memory Size HMS=5; Harmony memory consideration rate HMCR=0.95; Pitch adjustment rate PAR=0.25; Band width distance bw=0.02*(Ub- Lb).
Teaching Learning Based Optimization (TLBO)	Population Size N=20
Genetic Algorithm (GA)	Population size N=20, Mutation probability =0.2, Crossover probability =0.4, Number of bits =25.

The statistical and comparative analysis of the obtained results by the different selected optimization algorithms following the Friedman ranking test is presented in Table 2.

Table 2 Results of Friedman's statistical test of the optimization algorithms

Test Statistics		Algorithms	Mean Rank
Friedman's chi-square statistic	84	PSO	3
Degrees of freedom (df)	4	FBA	4
Number of observations N	21	HS	5
Standard Deviation (Sigma)	1.5811	TLBO	1
Prob>Chi-sq (P-value)	2.47e-17	GA	2

Based on the Friedman's statistical test, it shows that the difference between the performance of different proposed algorithms is significant, the level of probability (P) is very low and well below the critical value (P=0.05). Moreover, it was observed that the TLBO algorithm achieved the first rank with minimum simulation accuracy and could provide the best performance compared to other algorithms.

Consequently, the TLBO algorithm can be used to solve the optimization problems in the adopted methods for induced voltages calculation.
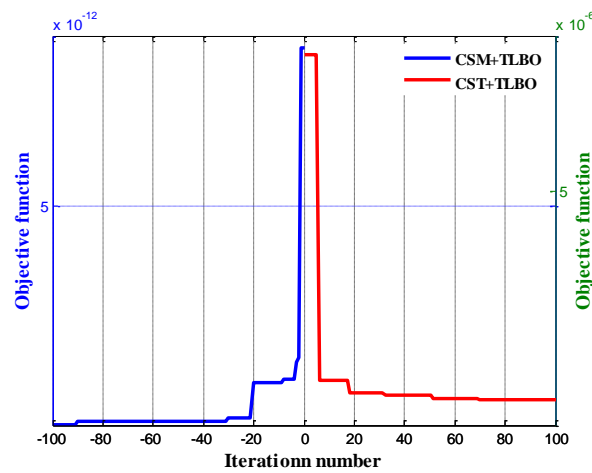
The variation of the objective functions (OF) mentioned in Equations (30 and 31) with the number of iterations is represented in Figure 10, it shows the search process adopted by this algorithm and the optimization based on the minimization of these objective functions. It can

be clearly observed that the objective functions values decrease as a number of iterations increase to converge towards a minimum solution.

The optimization results for the optimal values of the parameters to be inserted in these simulation methods are summarized in Table 3.

Table 3 Optimum Value of the Simulation Methods (CSM and CST)

| Algorithm+ Method		Phase conductor	Earth wire	Pipeline	OF value
CSM+ TLBO	Fictitious charges number	22	15	23	2e-14
	Fictitious radius [m]	0.036	0.008	0.14	
CST+ TLBO	Current filaments number	25	19	30	9.9e-07
	Fictitious radius [m]	0.03	0.01	0.1	

**Fig. 10** Objective functions variation with number of iterations

For electrostatic coupling analysis, Figure 11 shows the lateral profile of the electric field distribution with and without the presence of the metallic pipeline. It is clear from the graph that the initial electric field distribution is symmetrical at a distance of 7 m near the suspension pylon, the presence of the metallic pipeline has a relatively significant effect on the maximum value of the electric field at the exact location where this pipeline is located, at this point the electric field is subjected to a slight increase on the pipeline's surface due to the induced electrical charges accumulated on this surface. Therefore, it can be concluded that the presence of a metallic pipeline in the immediate vicinity of an overhead power line causes a distortion of the electric field at the emplacement where this pipeline is implanted.

The profile of the perturbed electric field on the pipeline's surface located at different distances in the two right-of-way sides is shown in Figure 12. It can be observed that the perturbed electric field reaches its maximum value (E= 7.12 kV/m) for a horizontal separation distance of pipeline equal to +7 m, as it gradually moves away from either side of this point, the electric field intensity begins to decline where it becomes almost minimal very far from the point of symmetry of the electric field. As a result, it is suggested that the

pipeline be located as far as possible from the power line in order to effectively reduce the electric field effects on this pipeline.
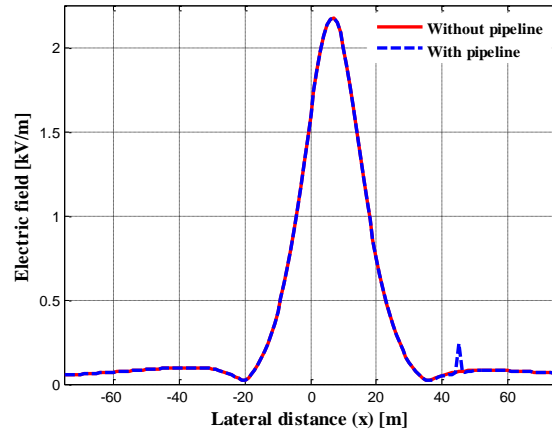
Fig. 11 Electric field profile with and without the metallic pipeline at 1 m above the ground
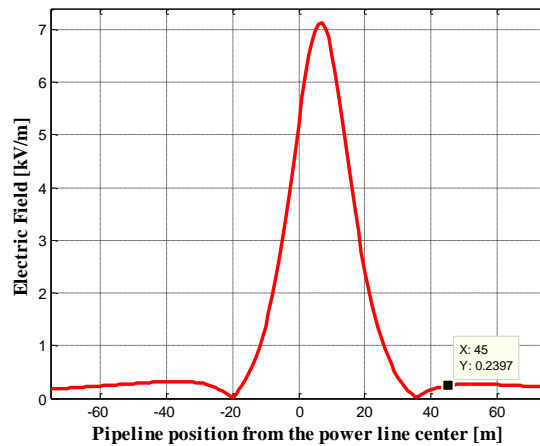

**Fig. 12** Perturbed electric field profile on the metallic pipeline's surface

Figure 13 shows the induced voltage profile on the pipeline's surface as a function of the separation distance of pipeline along the right-of-way. Generally, the voltage induced on the metallic pipeline is directly proportional to the perturbed electric field, its distribution is very similar to that of the perturbed electric field, the maximum value of the induced distance is obtained at a separation distance of pipeline equal to +7 m. As a general suggestion, it is highly recommended that the metallic pipeline be installed at a proximity distance called the critical distance where the induced voltage is below the values prescribed by international standards.

Under normal operating conditions, the discharge current due to the capacitive coupling through a person's body touching the metallic pipeline located at different separation distances

along the right of way is shown in Figure 14. It is important to note that the discharge current level is directly related to the induced voltage value, the higher induced voltage, the more intense in resulting current. The discharge current in this case study is 17 (mA), this value is considered unacceptable from a personnel safety point of view.
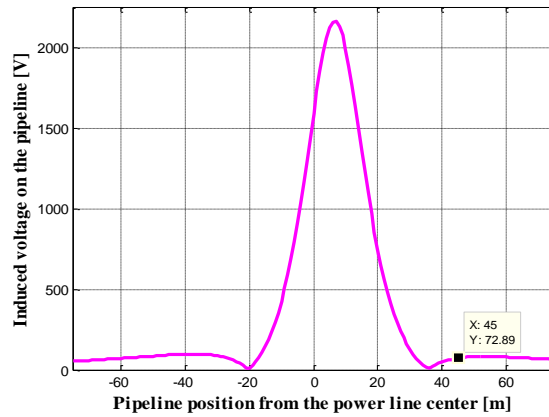

Fig. 13 Induced voltage on the insulated metallic pipeline due to HV power line
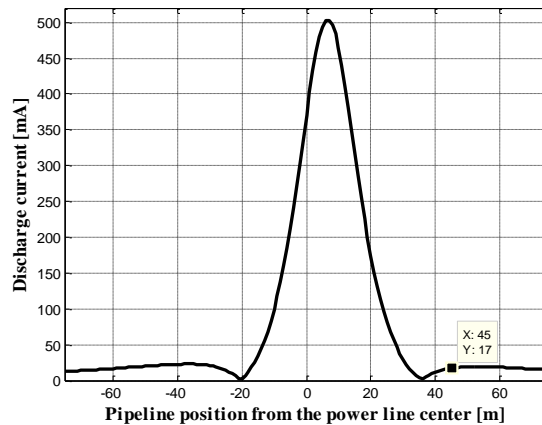

Fig. 14 Intensity of shock current flowing in human body

Concerning the discharge current values through the human body which are greater than the safety limit value recommended by the CIGRE standard which is equal to 10 mA. A protection procedure must be implemented, it is enough simply to connect the metallic pipeline to the earth through to an appropriate resistance calculated according to Equation (9). The grounding resistance of the pipeline as a function of its horizontal proximity distance is shown in Figure 15. As can be seen from this figure, the behavior of the graph represented by the grounding resistance is inversely to that of the discharge current. Therefore, the metallic pipeline in this study example is grounded by a very suitable resistance which is equal to 1429 Ω.
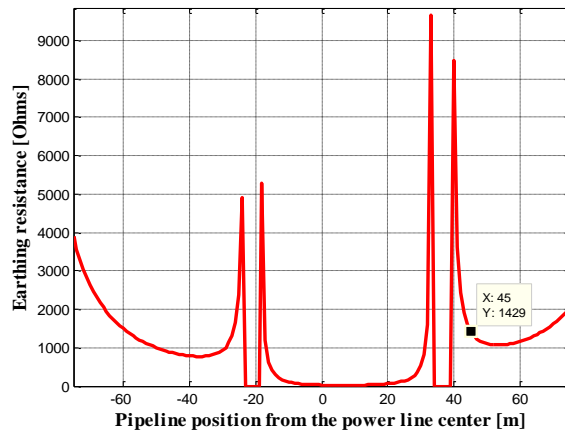
**Fig. 15** Calculation of the earthling resistance of metallic pipeline

For electromagnetic coupling analysis, Figure 16 shows the lateral profile of the magnetic induction distribution with and without the presence of the metallic pipeline, taking into account the effect of the induced currents in the earth wire and the metallic pipeline. Without the pipeline, it can be observed that the profile presents a symmetry close to the center of the power line (x = + 6 m), when it moves away from either side of this point, the magnetic induction intensity decreases rapidly as a function of the lateral distance. The figure also indicates, that the presence of a metallic pipeline in proximity to the power line disturbs the of magnetic induction distribution, this profile is distorted where the metallic pipeline is implanted. The pipeline will be affected by the magnetic induction and this is due to the current generated at the ends of this pipeline by the electromagnetic coupling.
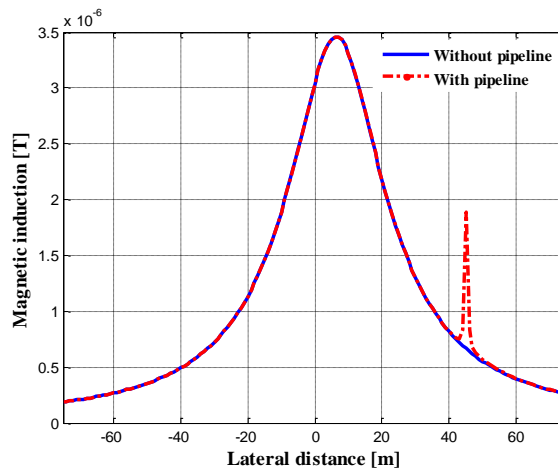
Fig. 16 Magnetic induction profile with and without the metallic pipeline at 1 m above
            the ground

The effect of the metallic pipeline's location along the right-of-way on the perturbed magnetic induction profile at its surface is shown in Figure 17. It can be seen that the

maximum value of the perturbed magnetic induction (B= 4.1 µT) is obtained directly near the lateral phase at a separation distance of pipeline equal to (x=+ 6 m), from this position the magnetic induction decreases continuously with the lateral metallic pipeline's location to reach less intense or lower values very far from the power line center.
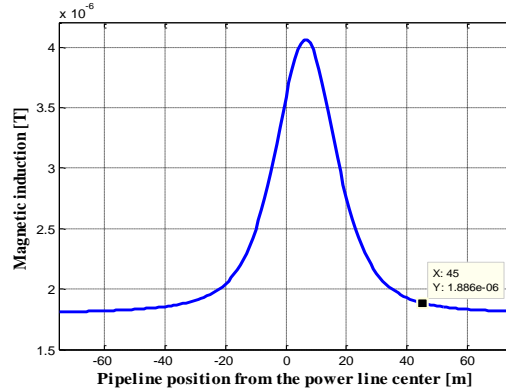
Fig. 17 Perturbed Magnetic induction profile on the metallic pipeline's surface

The induced voltage on the metallic pipeline by changing the pipeline's position along the right-of-way is shown in Figure 18. As can be seen in this figure that the induced voltage is maximum where the pipeline is located at proximity position equal to +6 m, then it decreases progressively as the lateral position of this pipeline increases in the two sides.

From this figure, it is important to note that the magnitude of the induced voltage in the metallic pipeline is directly proportional to the magnetic induction. In this case study the pipeline is kept location of 45 m from the pylon center, the obtained value of the induced voltage on the metallic pipeline is 270.9 V, this value is very higher than the maximum value permissible by the CIGRE norme which is 50 V.
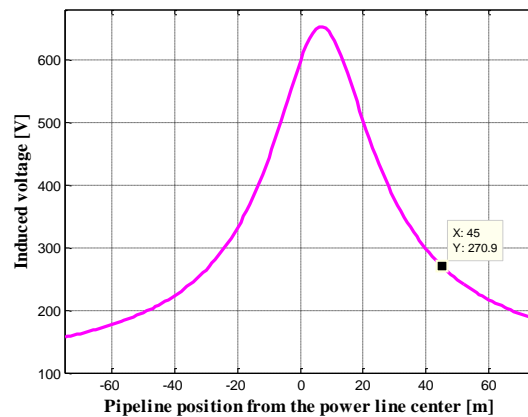
Fig. 18 Induced voltage profile on the metallic pipeline

The variation of the electric shock current flowing through a person coming into contact with the metallic pipeline as a function of its separation distance from the pylon is illustrated

in Figure 19. As reflected in this figure, the amount of the shock current that flow in the human body accidentally is perfectly proportional to the magnitude of the applied induced voltage on the metallic pipeline, the form of its graph is very similar to that of the induced voltage. In this case of study, during normal operation the shock current due to accidental contact with the metallic pipeline is 204.2 mA, which can cause a significant risk and a great severity for this human body by comparing it with the admissible body current.
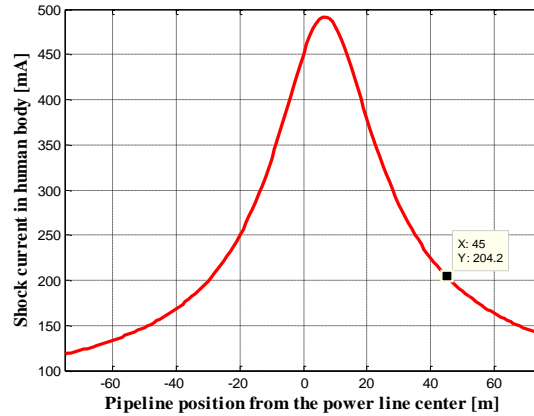

Fig. 19 Intensity of shock current flowing through the human body

For induced voltages values applied on the metallic pipeline which are greater than the maximum value admissible by the international CIGRE standard of 50V, that may pose a threat to the integrity of the pipeline and a risk to the safety of personnel. It then becomes imperative to implement an attenuation technique, to maintain the induced voltage at the recommended limit; it suffices simply to install low value shunt resistances at the ends of the pipeline with the earth which allow the current to be evacuated to earth along the pipeline section. Figure 20 shows the electrode resistance value as a function of the separation distance of the metallic pipeline, this graph illustrates the earthing resistance values that ensure the safety of personnel and metallic pipeline, the behavior of the earthing resistance profile is exactly opposite to that of the electric shock current.
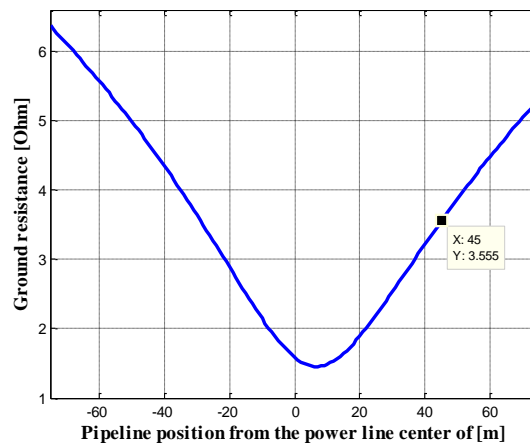

Fig. 20 Resistance of the ground electrode of metallic pipeline

Figure 21 shows the voltage applied to the electric system that combines in series the metallic pipeline and the electrode resistance to obtain a safety limit voltage (50 V). In this case study, it is necessary to install an earthing resistance value equal to 3.555 (Ω) at each end of the metallic pipeline.
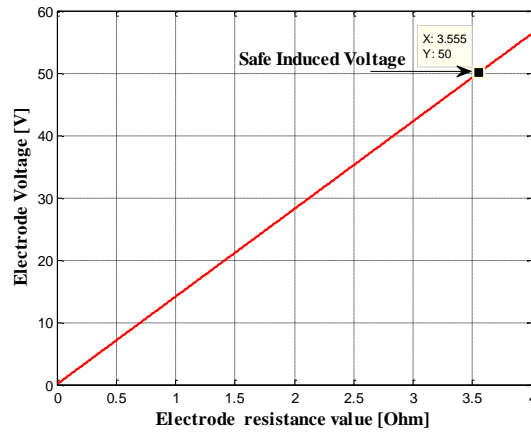

Fig. 21 Safe voltage in the electrode resistance

The results presented in Figures 22 and 23 show the combined effect due to the electrostatic and electromagnetic couplings, which is generally represented by the total induced voltage applied on the metallic pipeline, as well as the total discharge current passing through the human body. As can clearly see that the obtained values according to the position of the metallic pipeline along the right-of-way are very significant. They can constitute a serious danger for the safety of the agents of intervention and maintenance, a great threat for the pipeline integrity and perfect degradation following to the metal corrosion and damage of the applied coatings, the failure of the cathodic protection system and the various devices connected to the metallic pipeline. In order to protect the safety to personnel of intervention and maintenance, thus the cost-effective functioning of the metallic pipelines, the application of mitigation procedure is necessary.
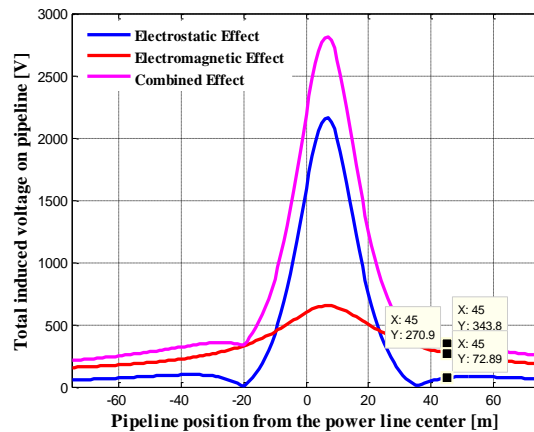
Fig. 22 Total Induced voltage on the metallic pipeline due to the combined effect
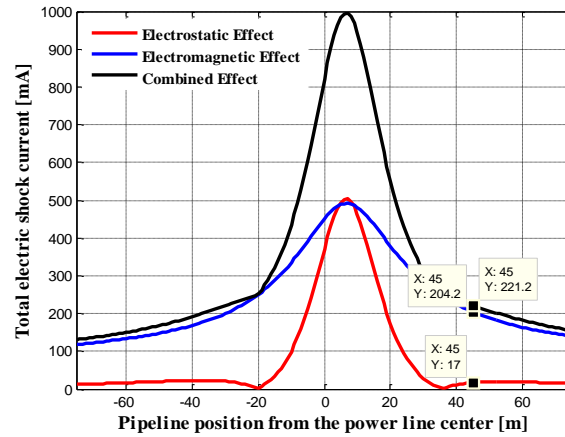
Fig. 23 Total shock current intensity flowing through the human body due to the combined effect

Finally, in order to verify the effectiveness of the proposed methods, the results obtained for the induced voltage intensity for the electrostatic and electromagnetic couplings were compared with those computed respectively by the approaches of admittance matrix analysis and Carson for the same data and similar geometry. Figures 24 and 25 show the comparisons between the values of the obtained induced voltage, the results analysis of the comparison indicates that there is a very good correlation between the graphs of the different methods, the maximum estimated relative errors between the values of these different methods according to the two couplings cases were within the permissible range, this process is sufficient to validate the precision of the methods adopted.
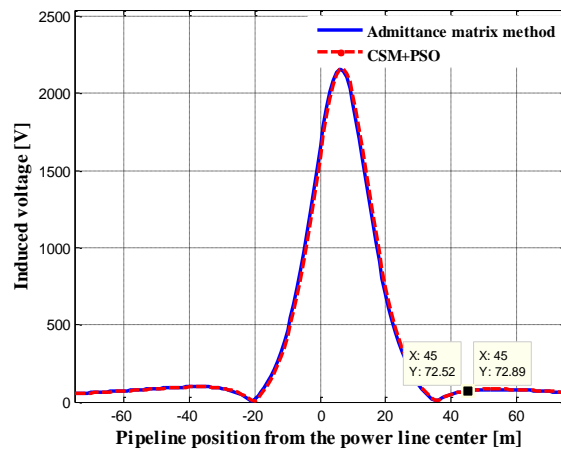
Fig. 24 Comparison of the induced values by the two calculation methods for electrostatic coupling
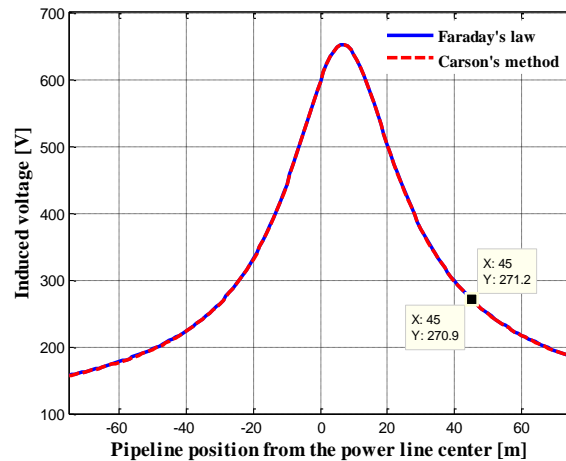
Fig. 25 Comparison of the induced values by the two calculation methods for electromagnetic coupling

8. CONCLUSION

In this paper, a rigorous quasi-static modeling approach is used to analyze the electrostatic and electromagnetic couplings under normal operating condition between an HV power transmission line and an aerial metallic pipeline placed in parallel and in close proximity. Two hybrid simulation methods based on the charge simulation (CSM) and current simulation techniques (CST), which are combined with the teaching learning based optimization (TLBO), were presented. This algorithm is applied in order to find the optimal position and the appropriate number of simulation charges and current filaments required of these methods. The intensities of the perturbed electric and magnetic fields and the induced voltage on the metallic pipeline were analyzed.

For electrostatic coupling, from the results, it is clear that the presence of an aerial metallic pipeline in the vicinity of HV overhead power transmission line causes the distortion of the electric field at pipeline's surface due to the resulting electric static charges accumulated on this insulated surface. The magnitude of the maximum value of the induced voltage on the pipeline occurs at a separation distance of 7 m, and then it declines rapidly on both sides of this distance, where it becomes almost negligible at a critical distance, at which it is recommended to lay this metallic pipeline. If the discharge current flowing in the human body during direct contact with the metallic pipeline exceeds the authorized safety limit, it is recommended that the mitigation procedure be installed and it is sufficient to ground the metallic pipeline with an appropriate resistance.

For electromagnetic coupling, according to the obtained results, it is evident that the presence of an aerial metallic pipeline in close proximity to a HV overhead power line disturbs the distribution of the magnetic field at the metallic pipeline's surface due to the electric current induced intensity in this pipeline. The maximum induced voltage appears in the metallic pipeline is obtained when this pipeline is located at a proximity distance equal to + 6 m from the pylon, then it decreases rapidly with the increase of the separation distance of the metallic pipeline across the sides of pylon.

The amount of discharge current which passes through the human body when it accidentally touches the metallic pipeline is linearly proportional to the magnitude of the induced voltage. When the resultant of the induced voltage intensity on the metallic pipeline exceeds the safety threshold of 50 V, it can present risks for the safety of intervention and maintenance agents, also for the pipeline's equipments, these risks can be completely eliminated by applying the mitigation measure, it be sufficient to connect the two endings of the metallic pipeline to the earth through a suitable resistances.

The numerical results presented by the hybrid developed methods are compared with the results obtained by two different approaches, concerning respectively the both studied couplings; the comparison shows a good agreement between the simulation results, which confirms the efficiency and the validity of the proposed methods.

REFERENCES

[1]   CIGRE, *Guide on the Influence of High Voltage AC Power Systems on Metallic Pipelines*, Working Group 36.02, Technical Brochure No. 095, 1995.

[2]   R. A. Gummow, *A/C Interference Guideline Final Report*, Nace Corrosion Specialist, No.17, Canadian Energy Pipeline Association, 2014.

[3]   EN 50443, *effects of electromagnetic interference on pipelines cased by high voltage A.C. railway systems and/or high voltage A.C. power supply systems*, CENELEC Report No: ICS 33.040.20; 33.100.01, 2009.

[4]   Australian New Zealand Standard, *Electrical Hazards on Metallic Pipelines*, Standards Australia, Standards New Zealand, 4853:2000.

[5]   D. D. Micu, E. Simion, D. Micu and A. Ceclan, "Numerical methods for induced voltage evaluation in electromagnetic interference problems", In Proceedings of the 9th International Conference on Electrical Power Quality and Utilisation, 2007, pp. 1–6.

[6]   K. Hyoun-Su, H. Y. Min, J. G. Chase and C. H. Kim, "Analysis of Induced Voltage on Pipeline Located Close to Parallel Distribution System", *Energies*, vol. 14, pp. 8536–8536, 2021.

[7]   J. Dabkowski, "How to predict and mitigate A.C. Voltages on buried pipelines", *Pipeline & Gas J.*, vol. 206, pp. 19–21, 1979.

[8]   A. Taflove and J. Dabkowski, "Prediction Method for Buried Pipeline Voltages Due to 60 Hz AC Inductive Coupling Part I - Analysis", *IEEE Trans. Power Apparatus and Systems.*, vol. PAS-98, no. 3, pp. 780–787, 1979.

[9]   J. Dabkowski, "The Calculation Magnetic Coupling from Overhead Transmission Lines", *IEEE Trans. Power Appar. Syst.*, vol. PAS-100, no. 8, pp. 3850–3860, 1981.

[10] F. P. Dawalbi and R. D. Southey, "Analysis of Electrical Interference from Power Lines to Gas Pipelines Part I: Computation Methods", *IEEE Power Eng. Rev.*, vol. 9, no. 7, pp.70–70, 1989.

[11] F. P. Dawalibi and R. D. Southey, "Analysis of electrical interference from power lines to gas pipelines. II. Parametric analysis", *IEEE Trans. Power Deliv.*, vol. 5, no. 1, pp. 415–421, 1990.

[12] G. Djogo and M. M. A. Salama, "Calculation of inductive coupling from power lines to multiple pipelines", *Electr. Power Syst. Res.*, vol. 41, no. 1, pp. 75–84, 1997.

[13] D. D. Micu, G. C. Christoforidis and L. Czumbil, "AC interference on pipelines due to double circuit power lines: A detailed study", *Electr. Power Syst. Res.*, vol. 103, pp. 1–8, 2013.

[14] A. Muresan, T. A. Papadopoulos, L. Czumbil, A. I. Chrysochos, T. Farkas and D. Chioran, "Numerical Modeling Assessment of Electromagnetic Interference between Power Lines and Metallic Pipelines: A Case Study", In Proceedings of the 9th International Conference on Modern Power Systems. Cluj-Napoca, 2012, pp. 1–6.

[15] R. Djekidel and D. Mahi, "Calculation and analysis of inductive coupling effects for HV transmission lines on aerial pipelines", *Przegląd Elektrotechniczny.*, vol. 190, no.9, pp. 151–156, 2014.

[16] L. Li and X. Gao, "AC corrosion interference of buried long distance pipeline", In Proceedings of the 3rd International Conference on Intelligent Control-Measurement and Signal Processing and Intelligent Oil Field. Xi'an, 2012, pp. 342–346.

[17] K. J. Satsios, D. P. Labridis and P. S. Dokopoulos, "Finite Element Computation of Field and Eddy Currents of a System Consisting of a Power Transmission Line Above Conductors Buried in Nonhomogeneous Earth", *IEEE Trans. Power Deliv.*, vol. 13, no. 3, pp. 876–882, 1998.

[18] A. Cristofolini, A. Popoli and L. Sandrolini, "Numerical Modelling of Interference from AC Power Lines on Buried Metallic Pipelines in Presence of Mitigation Wires", In Proceedings of the 2018 IEEE

International Conference on Environment and Electrical Engineering and 2018 IEEE Industrial and Commercial Power Systems Europe, Palermo, 2018, pp. 1–5.

[19] A. Popoli, L. Sandrolini and A. Cristofolini, "Finite Element Analysis of Mitigation Measures for AC Interference on Buried Pipelines", In Proceedings of the IEEE International Conference on Environment and Electrical Engineering and Industrial and Commercial Power Systems Europe, Genova, 2019, pp. 1–5.

[20] A. Popoli, A. Cristofolini, L. Sandrolini, B. T. Abe and A. Jimoh, "Assessment of AC interference caused by transmission lines on buried metallic pipelines using F.E.M," In Proceedings of the 2017 International Applied Computational Electromagnetics Society Symposium, Firenze, 2017, pp. 1–2.

[21] N. Abdullah, "HVAC interference assessment on a buried gas pipeline", *IOP Conf. Series: Earth and Environ. Sci.*, vol. 704, no. 1, pp. 012009, 2021.

[22] G. C. Christoforidis, P. S. Dokopoulos and K. E. Psannis, "Induced voltages and currents on gas pipelines with imperfect coatings due to faults in a nearby transmission line", In Proceedings of the IEEE International Conference on Porto Power Tech. Porto, 2001, pp. 401–406.

[23] G. C. Christoforidis and D. P. Labridis, "Inductive Interference of Power Lines on Buried Irrigation Pipelines", In Proceedings of the IEEE International Conference of Power, Bologna, 2003, pp. 196–202.

[24] G. C. Christoforidis, D. P. Labridi and P. S. Dokopoulos, "A hybrid method for calculating the inductive interference caused by faulted power lines to nearby buried pipelines", *IEEE Trans. Power Deliv.*, vol. 20, no. 2, pp. 1465–1473, 2005.

[25] A. Popoli, A. Cristofolini and L. Sandrolini, "A numerical model for the calculation of electromagnetic interference from power lines on nonparallel underground pipelines", *Math. Comput. Simul.*, vol. 183, pp. 221–233, 2021.

[26] C. Andrea, A. Popoli, L. Sandrolini, G. Pierotti and M. Simonazzi, "Laplace Transform for Finite Element Analysis of Electromagnetic Interferences in Underground Metallic Structures", *Appl. Sci.*, vol. 12, no. 2, pp. 872–872, 2022.

[27] H. G. Lee, T. H. Ha, Y. C. Ha, J. H. Bae and D. K. Kim, "Analysis of voltages induced by distribution lines on gas pipelines," In Proceedings of the IEEE International Conference on Power System Technology. Singapore, 2004, pp. 598–601.

[28] S. Al-Alawi, A. Al-Badi and K. Ellithy, "An artificial neural network model for predicting gas pipeline induced voltage caused by power lines under fault conditions", *Int. J. Comput. Math. Electr. Electron. Eng.*, vol. 24, no. 1, pp. 69–80, 2005.

[29] A. Popoli, L. Sandrolini and A. Cristofolini, "Comparison of screening configurations for the mitigation of voltages and currents induced on pipelines by HVAC power lines", *Energies J.,* vol. 14, pp. 3855–3855, 2021.

[30] M. A. Elhirbawy, L. S. Jennings, S. M. AI Dhalaan and W. W. L. Keerthipala, "Practical Results and Finite Difference Method to Analyze the Electric and Magnetic Field Coupling Between Power Transmission Line and Pipeline", In Proceedings of the IEEE International Symposium on Circuits and Systems, 2003, pp. 431–434.

[31] Mazen Abdel-Salam, Abdallah Al-Shehri, "Induced Voltages on Fence Wires and Pipelines by AC Power Transmission Lines", *IEEE Trans. Ind. Appl.*, vol. 30, no. 2, pp. 341–349, 1994.

[32] M. M. Saied, "The Capacitive Coupling between EHV Lines and Nearby Pipelines", *IEEE Trans Power Deliv.*, vol. 19, no. 3, pp. 1225–1231, 2004.

[33] A. Gupta and M. J. Thomas, "Coupling of high voltage AC power line fields to metallic pipelines", In Proceedings of the 9th IEEE International Conference on Electromagnetic Interference and Compatibility (INCEMIC 2006), Bangalore, 2006, pp. 278–283.

[34] H. M. Ismail, A. M. Amin and S. Alkhoudary, "Comparative study of the effect of HVTL Electrostatic fields on gas pipelines using the ATP-LCC& CSM methods", *Int. J. Eng. Res. Technol.*, vol. 2, no. 9, pp. 3037–3043, 2013.

[35] R. Djekidel and S. A. Bessidek, "Estimation and Mitigation of Electrostatic Interferences on Metallic Pipeline by HV Overhead Power Line using Differential Evolution Algorithm", *Electrotehnica, Electronica, Automatica EEA*, vol. 64, no. 3, pp. 83–90, 2016.

[36] R. Djekidel, S. A. Bessedik and A. Hadjadj, "Electric field modeling and analysis of EHV power line using improved calculation method", *FU Electr. Energ.*, vol. 31, no. 3, pp. 425–445, 2018.

[37] R. Djekidel, S. A. Bessedik and S. Akef, "Accurate computation of magnetic induction generated by HV overhead power lines", *FU Electr. Energ.*, vol. 32, no. 2, pp. 267–285, 2019.

[38] T. Meriouma, S. A. Bessedik and R. Djekidel, "Modelling of Electric and Magnetic Field Induction under Overhead Power Line using Improved Simulation Techniques", *Eur. J. Electr. Eng.*, vol. 23, no. 4, pp. 289–300, 2021.

[39] R. V. Rao, V. J. Savsani and D. P. Vakharia, "Teaching–learning-based optimization: a novel method for constrained mechanical design optimization problems", *Comput. Aided Des. J.*, vol. 43, no. 3, pp. 303–315, 2011.

[40] S. Li, W. Gong, L. Wang, X. Yan and C. Hu, "A hybrid adaptive teaching–learning-based optimization and differential evolution for parameter identification of photovoltaic models", *Energy Convers. Manag.*, vol. 225 p. 113474, 2020.

[41] N. H. Malik, "A review of the charge simulation method and its applications," *IEEE Trans. Electr. Insul.,* vol. 24, no. 1, pp. 3–20, 1989.

[42] F. Lai, Y. Wang, Y. Lu and J. Wang, "Improving the Accuracy of the Charge Simulation Method for Numerical Conformal Mapping", *Math. Probl. Eng.*, vol. 2017, p. 3603965, 2017.

[43] R. Djekidel and D. Mahi, "Effect of the Shield Lines on the Electric Field Intensity around the High Voltage Overhead Transmission Lines", *AMSE Journals -Series: Modelling A.*, vol. 87; no. 1, pp. 1–16, 2014.

[44] R. Djekidel, D. Mahi and A. Ameur, "Analysis of Parameters Affecting the Capacitive Interference between Pipelines and Power Overhead Line Using Genetic Algorithms", *Int. J. Electr. Eng. Inform.*, vol. 8, no. 2, pp. 315–330, 2016.

[45] R. Djekidel, "Optimum Phase Configuration and Location of the Aerial Pipeline in the Vicinity of a High Voltage Overhead Line", *Period. Polytech. Electr. Eng. Comput. Sci.*, vol. 60, no. 2, pp. 143–150, 2016.

[46] R. M. Radwn and M. M. Samy, "Calculation of Electric Fields underneath Six Phase Transmission Lines," *J. Electr. Syst.*, vol. 12, no. 4, pp. 839–851, 2016.

[47] M. M. Samy and A. M. Emam, "Computation of electric fields around parallel HV and EHV overhead transmission lines in Egyptian power network", In Proceedings of the IEEE International Conference on Environment and Electrical Engineering and IEEE Industrial and Commercial Power Systems Europe, Italy, 2017, pp. 1– 5.

[48] Y. Wang and C. Lv, "Electric Field Calculation of the Improved Charge Simulation Method Based on Hybrid Coding", *Chinese Automation Congress*, pp. 1208–1213, 2019.

[49] S. Nakasumi, K. Kikunaga, Y. Harada, M. Ohkubo and K. Takagi, "Error evaluation of defect shape identification using charge simulation method for static electricity", *J. Electrostatics.*, vol. 114, p. 103633, 2021.

[50] R. Djekidel, S. A. Bessedik and A. C. Hadjadj, "Assessment of electrical interference on metallic pipeline from HV overhead power line in complex situation*", FU Electr. Energ.*, vol. 34, no. 1, pp. 53–69, 2021.

[51] R. Djekidel, A. Choucha and A. C. Hadjadj, "Efficiency of some optimization approaches with the charge simulation method for calculating the electric field under extra high voltage power lines," *IET Gener. Transm. Distrib.*, vol. 11, no. 17, pp. 4167–4174, 2017.

[52] F. Yang, W. He, W. Deng and T. Chen, "A genetic algorithm-based improved charge simulation method and its application", *Int. J. Comput. Math. Electr. Electron. Eng.*, vol. 28, no. 6, pp. 1701–1709, 2009.

[53] R. Wang, J. Tian, F. Wu, Z. Zhang and H. Liu, "PSO/GA Combined with Charge Simulation Method for the Electric Field Under Transmission Lines in 3D Calculation Model", *Electronics*, vol. 8, no. 10, pp. 1140, 2019.

[54] N. Tleis, *Power Systems Modeling and Fault Analysis Theory and Practice*, Elsevier, Second Edition 2019, pp. 835–861.

[55] IEEE Std 80-2013, *IEEE Guide for Safety in AC Substation Grounding*, (Revision of IEEE Standard 80-2000), 2013, pp. 1-226.

[56] Y. Degui, L. Bing, D. Jun, H. Danmei and W. Xihong, "Power Frequency Magnetic Field of Heavy Current Transmit Electricity Lines Based on Simulation Current Method", *IEEE World Autom. Congr.*, pp. 1–4, 2008.

[57] R. Roshdy, A. S. Mazen, M. Abdel-Bary and S. Mohamed, "Laboratory Validation of Calculations of Magnetic Field Mitigation Underneath Transmission Lines Using Passive and Active Shield Wires", *Innovative Syst. Des. Eng.*, vol. 2, no. 4, pp. 218–232, 2011.

[58] R. M. Radwan, M. Abdel-Salam, M. M. Samy and A.M. Mahdy, "Passive and active shielding of magnetic fields underneath overhead transmission lines theory versus experiment", In Proceedings of the 17th International Middle East Power Systems Conference. Mansoura, 2015, pp. 1–10.

[59] M. Abdel-Salam, H. Abdullah, M. Th. El-Mohandes and H. El-Kishky, "Calculation of magnetic fields from electric power transmission lines", *Electr. Power Syst. Res.*, vol. 49, pp. 99–105, 1999.

[60] M. Albano, R. Turri, S. Dessanti, A. Haddad and H. Griffiths, B. Howat, "Computation of the electromagnetic coupling of parallel untransposed power lines", In Proceedings of the 41st International Universities Power Engineering Conference. Newcastle upon Tyne, 2006, pp. 303–307.

[61] R. Djekidel, S. A. Bessedik, P. Spitéri and D. Mahi, "Passive mitigation for magnetic coupling between HV power line and aerial pipeline using PSO algorithms optimization", *Electr. Power Syst. Res.*, vol. 165, pp.18–26, 2018.

[62] K. Yamazaki, T. Kawamoto and H. Fujinami, "Requirements for Power Line Magnetic Field Mitigation Using a Passive Loop Conductor", *IEEE Trans. Power Deliv.*, vol. 15, no. 2, pp. 646–651, 2000.

[63] P. Cruz, C. Izquierdo and M. Burgos, "Optimum passive shields for mitigation of power lines magnetic field", *IEEE Trans. Power Deliv.*, vol. 18, no. 4, pp. 1357–1362, 2003.

[64] A. R. Memari, "Optimal calculation of impedance of an auxiliary loop to mitigate magnetic field of a transmission line", *IEEE Trans. Power Deliv.*, vol. 20, no. 2, pp. 844–850, 2005.

[65] D. Tang, J. Zhao and H. Li, "An Improved TLBO algorithm with Memetic method for Global Optimization", *Int. J. Adv. Comput. Technol.*, vol. 5, no. 9, pp. 942–949, 2013.

[66] H. R. E. H. Bouchekara, M. A. Abido and M. Boucherma, "Optimal Power flow using Teaching learning based optimization", *Electr. Power Syst. Res.*, vol. 114, pp. 49–59, 2014.

[67] P. Sarzaeim, O. B. Haddad and X. Chu, *Teaching-Learning-Based Optimization (TLBO) Algorithm. In: Advanced Optimization by Nature-Inspired Algorithms. Studies in Computational Intelligence*, Springer, Singapore, vol. 720, pp. 51–58, 2018.

[68] M. M. Puralachetty, V. K. Pamula, L. M. Gondela, V. N. B. Akula, "Teaching-learning-based optimization with two-stage initialization", In Proceedings of the IEEE Students' International Conference on Electrical, Electronics and Computer Science. Bhopal, 2016, pp. 1–5.

[69] R. Venkata-Rao, V. Patel, "An improved teaching-learning-based optimization algorithm for solving unconstrained optimization problems", *Scientia Iranica*., vol. 20, no. 3, pp. 710–720, 2013.

[70] O. Bozorg-Haddad, P. Sarzaeim and H. A. Loáiciga, "Developing a novel parameter-free optimization framework for flood routing", *Sci. Rep.*, vol. 11, no. 1, p. 16183, 2021.

[71] R. Venkata-Rao and V. Patel, "An elitist teaching-learning-based optimization algorithm for solving complex constrained optimization problems," *Int. J. Ind. Eng. Comput.*, vol. 3, no. 4, pp. 535–560, 2012.

[72] X. He, J. Huang, Y. Rao and L. Gao, "Chaotic Teaching-Learning-Based Optimization with Lévy Flight for Global Numerical Optimization", *Comput. Intell. Neurosci.*, vol. 8341275, pp. 1687–5265, 2016.

[73] S. Sleesongsom and S. Bureerat, "Four-bar linkage path generation through self-adaptive population size teaching-learning based optimization", *Knowledge-Based Syst.*, vol. 135, pp. 180–191, 2017.

[74] T. Hastie, R. Tibshirani and J. Friedman, *the Elements of Statistical Learning: Data Mining, Inference, and Prediction*. New York: Springer, Second Edition 2009, pp.745.

[75] D. Joaquin, G. Salvador, M. Daniel, H. Francisco, "A practical tutorial on the use of nonparametric statistical tests as a methodology for comparing evolutionary and swarm intelligence algorithms", *Swarm Evol. Comput.*, vol. 1, no.1, pp. 3–18, 2011.

[76] M. A. El-Shorbagy and A. Y. Ayoub, "Integrating Grasshopper Optimization Algorithm with Local Search for Solving Data Clustering Problems", *Int. J. Comput. Intell. Syst.*, vol. 14, no. 1, pp. 783–793, 2021.

[77] H. Moayedi, H. Nguyen and L. Kok-Foong, "Nonlinear evolutionary swarm intelligence of grasshopper optimization algorithm and gray wolf optimization for weight adjustment of neural network", *Eng. with Comput.*, vol. 37, no. 2, pp. 1265–1275, 2021.

[78] W. Li, Y. Fan and Q. Xu, "Teaching-Learning-Based Optimization Enhanced With Multiobjective Sorting Based and Cooperative Learning", *IEEE Access J.*, vol. 8, p. 65937, 2020.

[79] M. M. Samy, S. Barakat and H. S. Ramadan, "A Flower Pollination Optimization Algorithm for an Off-Grid PV-Fuel Cell Hybrid Renewable System", *Int. J. Hydrog. Energy*, vol. 44, no. 4, pp. 2141–2152, 2019.

[80] N. Sinsuphan, U. Leeton and T. Kulworawanichpong, "Optimal power flow solution using improved harmony search method," *Appl. Soft Comput. J.*, vol. 13, no. 5, pp. 2364–2374, 2013.

[81] S. Shabir and R. Singla, "A Comparative Study of Genetic Algorithm and the Particle Swarm Optimization", *Int. J. Electr. Eng.*, vol. 9, no. 2, pp. 215–223, 2016.

[82] M. H. Shwehdi, M. A. Alaqil and S. Mohamed, "EMF analysis for a 380 kV transmission OHL in the vvicinity of buried pipelines", *IEEE Access J.*, vol. 8, pp. 3710–3717, 2020.

[83] R. Djekidel and D. Mahi, "Capacitive interferences modelling and optimization between HV power lines and aerial pipelines", *Int. J. Electr. Comput. Eng.*, vol. 4, no. 4, pp. 486–497, 2014.

[84] M. Samy and A. Emam, "Induced pipeline voltage nearby hybrid transmission lines", *Innovative Syst. Des. Eng.*, vol. 8, no. 3, pp. 31–40, 2017.

[85] R. Djekidel, A. Hadjadj and S. A. Bessedik, "Electrostatic and electromagnetic effects of HV overhead power line on above metallic pipeline", In Proceedings of the 5th IEEE International Conference on Electrical Engineering, Boumerdes, 2017, pp. 1–6.

[86] K. B. Adedeji, "Effect of HVTL Phase Transposition on Pipelines Induced Voltage", *Indones. J. Electr. Eng. Inform.*, vol. 4, no. 2, pp. 93–101, 2016.

[87] A. Hellany, M. Nassereddine and M. Nagrial, "Analysis of the impact of the OHEW under full load and fault current", *Int. J. Energy Environ.*, vol. 1, no. 4, pp. 727–736, 2010.

[88] M. Nassereddine and A. Hellany, "AC Interference Study on Pipeline: The Impact of the OHEW under Full Load and Fault Current", In Proceedings of the 2nd IEEE International Conference on Computer and Electrical Engineering, Dubai, 2009, pp. 497–501.

[89] K. B. Adedeji, A. A. Ponnle, B. T. Abe, A. A. Jimoh, A. M. I. Abu-Mahfouz and Y. Hamam, "GUI-based AC induced corrosion monitoring for buried pipelines near HVTLs", *Eng. Letters.*, vol. 26, no. 4, pp. 489–497, 2018.

[90] M. Vakilian, K. Valadkhani, A. Shaigan, A. Nasiri and H. Gharagozlo, "A method for evaluation and mitigation of AC induced voltage on buried gas pipelines", *Scientia Iranica*, vol. 9, no. 4, pp. 311–320, 2002.